

Surface and Grain Boundary Segregation of Antimony and Tin - Effects on Steel Properties

Segregacija antimona in kositra na površini in po mejah zrn - vpliv na lastnosti jekel

H. J. Grabke¹, Max-Planck-Institut, Düsseldorf, Germany

Dedicated to Prof. Dr. F. Vodopivec on the occasion of his 65th birthday.
Prof. dr. Francu Vodopivcu za njegov 65. rojstni dan.

Prejem rokopisa - received: 1996-10-01; sprejem za objavo - accepted for publication: 1996-11-04

The tramp elements Sb and Sn have a strong tendency to surface segregation on iron. By LEED and AES surface structures and concentrations of Sb and Sn segregated on single crystal were determined. The surface segregation is strongly dependent on orientation, therefore recrystallization of steel sheet is affected since the surface energies of different grains are reduced to different extent - this effect may be used to obtain advantageous textures of electrical steel sheet and deep drawing steels. Surface segregation of Sb and Sn retards surface reaction kinetics as was shown for the gas carburization of case hardening steels. Surface segregation of tin in creep cavities of turbine steels was shown to accelerate the creep fracture. The grain boundary segregation of both elements in iron is minor, and furthermore Sb and Sn are displaced from grain boundaries by carbon so that most steels are not endangered by grain boundary embrittlement due to Sb and Sn, but some low alloy turbine steels are susceptible to temper and long-term embrittlement.

Key words: surface and grain boundary segregation Fe-Sb alloys, Fe-Sn alloys, Fe-Sb-C alloys, Fe-Sn-C alloys, intergranular fracture embrittlement

Elementa v sledeh Sb in Sn močno segregirata na površini železa. Površinska struktura in koncentracija Sb in Sn v segregirani plasti sta bili določeni z metodami LEED in AES. Površinska segregacija je odvisna od kristalografske orientacije, rekristalizacija jeklenih pločevin je aktivirana, ker imajo posamezna kristalna zrna različno znižano površinsko energijo - pojav se lahko uporabi za pridobivanje prednostnih tekstur elektro pločevin in pločevin za globoki vlek. Površinska segregacija Sb in Sn zavira kinetiko površinske reakcije kar je prikazano pri procesu naogljčevanja jekel. Površinska segregacija kositra v vdolbinah pri lezenju jekel za turbine povzroča pospešenje lezenja do preloma. Segregacija obeh elementov po mejah kristalnih zrn je v železu minimalna zato ker Sb in Sn na mejah zrn izpodrine ogljik. Tako večina jekel ni ogroženih zaradi krhkosti kristalnih mej, ki bi jih povzročala Sb in Sn, le nekatera nizka ogljična turbinska jekla so občutljiva na popuščno krhkost.

Ključne besede: površinska segregacija, segregacija po mejah zrn, Fe-Sb zlitine, Fe-Sn zlitine, Fe-Sb-C, Fe-Sn-C, interkristalna krhkost

1 Introduction

1.1 The role of tramp elements in steels

The effects of the so-called tramp elements in steels, Ni, Cu, P, S, Pb, As, Sb, Sn etc. are generally deleterious, the greatest problems they cause are 'hot shortness' and 'temper embrittlement' of steels. The hot shortness, a lack of hot workability can have different reasons, one possible reason is the copper enrichment due to surface scaling^{1,2}. Beneath the scale the more noble elements Cu, As, Sb, Sn are enriched and form a liquid phase which causes surface cracking by grain boundary penetration. Sb and Sn greatly reduce the solubility of Cu in austenite and hence lead to precipitation of a molten phase and its grain boundary penetration, under conditions of much less enrichment and down to lower temperatures. The enrichment of tramp elements below the oxide scale upon reheating or hot rolling of steels and could be detected by electron microprobe (EPMA). This enrichment also can have strong effects on the scale adherence and mor-

phology as has been studied extensively by F. Vodopivec et al. in work started at the IRSID³⁻¹¹: by the presence of the more noble elements Cu, Ni, Sb, Ag, S the scale adherence is enhanced whereas the elements Si, Al, P and B which are oxidized and form silicate, aluminate, phosphate or borate layers cause formation of voids and cavities at the scale/metal interface.

The other way of enrichment which leads to deleterious effects of tramp elements is equilibrium segregation, so the 'temper embrittlement' is caused by segregation of P, Sn or Sb in the temperature range 400 - 700°C to the steel grain boundaries, e.g. during slow cooling after tempering, but also during application of steels in this temperature range. It was suspected since long that temper embrittlement is caused by grain boundary segregation, but this suspect could be confirmed only after the arrival and spreading of interfacial analysis by Auger-electron spectroscopy (AES) in the eighties. But the tramp elements do not have only deleterious effects, e.g. it is known that Cu can enhance the resistance against atmospheric corrosion. Even positive effects of Sb and Sn were detected and studied at the IMT Ljubljana and the MPI für Eisenforschung Düsseldorf¹²⁻²⁰, these tramp elements can improve the texture and magnetic proper-

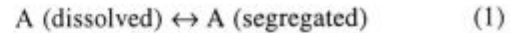
¹ Prof. Dr. Sc. Hans Jürgen GRABKE
Max-Planck-Institut für Eisenforschung GmbH
Postfach 140444, 40074 Düsseldorf, Germany

ties of nonoriented silicon steel sheets, caused by surface segregation and its effect on surface energies as discussed in the following chapter.

1.2 Fundamentals of surface and grain boundary segregation

In this review the equilibrium segregation of Sb and Sn will be described and only the effects will be discussed which are caused by equilibrium surface and grain boundary segregation. Most elements which are dissolved in iron tend to enrich at elevated temperatures at surfaces, grain boundaries and interfaces²¹⁻²⁵, and dis-

tribution equilibria are established at sufficiently high temperature.



There are different driving forces for such equilibrium segregation:

1. free bonds at the surface or interface can be saturated by interaction with the atoms A
2. the iron surface may be covered with a layer of atoms A which has a lower surface energy than the initial iron surface
3. the release of atoms A from the bulk solution leads to release of elastic energy, especially in the case of in-

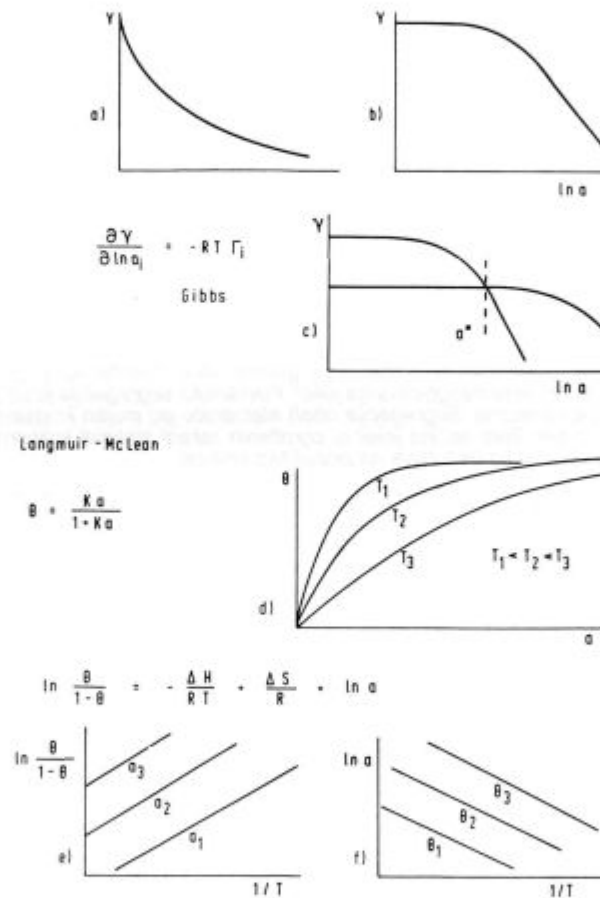


Figure 1: Schematic diagrams on the Gibbs isotherm (a-c) and the Langmuir-McLean isotherm (d-f)
 a) surface energy γ vs activity a of the adsorbed or segregated element A,
 b) γ vs $\ln a$ and
 c) the latter plot for two orientations with different surface energies and different adsorption or segregation behaviour - upon increasing activity a and coverage θ the surface firstly instable becomes stable, a reason for tertiary recrystallization or faceting,
 d) degree of coverage θ vs activity of the adsorbed or segregated element A,
 e) plot for the evaluation of studies at constant activity or concentration of the element A,
 f) isosteres for determination of the thermodynamic data at constant coverage

Slika 1: Shematski diagrami Gibbsove izoterme (a-c) in Langmuir-McLeanove izoterme (d-f)
 a) površinska energija γ v odvisnosti od aktivnosti a adsorbiranega ali segregiranega elementa A, b) γ v odvisnosti od $\ln a$ in
 c) zadnji grafikon za dve orientaciji z različnimi površinskimi energijami in različno adsorbicijo oziroma segregacijo - po zvišanju aktivnosti a in pokritja θ je sprva nestabilna površina postala stabilna, vzrok za terciarno rekristalizacijo ali facetiranje,
 d) stopnja pokritja θ v odvisnosti od adsorbiranega ali segregiranega elementa A,
 e) grafični prikaz za ovrednotenje študij pri konstantni aktivnosti ali koncentraciji elementa A,
 f) izostere za določitev termodinamičnih podatkov pri konstantnem številu atomov A

terstitial atoms or substitutional atoms larger than the iron atoms.

The latter effect is certainly true for Sb and Sn since both elements have large atoms, causing a strain in the iron lattice and increase of lattice parameter²⁶. In fact, all equilibrium segregation processes should lead to a decrease in surface energy (or interfacial energy) according to Gibbs' law

$$\frac{d\gamma}{d \ln a_A} = -RT \Gamma_A \quad (2)$$

where γ is the surface energy, a_A the thermodynamic activity of the segregating species A and Γ_A the surface concentration (mol/cm²), R gas constant, T temperature (K) (Figure 1a-c). The effect of adsorption or segregation on surface energy can be measured by the so-called zero creep method²⁷ but only at very high temperatures. One example of the result for a measurement on Fe-Sn foils with different Sn concentrations at 1420°C^{28,29} is given in Figure 2a. Combining such a study with measuring 'grain boundary grooving', i.e. the dihedral angle of the thermally etched grain boundary grooves at the surface gave the ratio of the grain boundary to surface energies and thus the dependence of grain boundary energy was derived as a function of the bulk tin content (Figure 2b). From these 'Gibbs isotherms' also the isotherms for surface resp. grain boundary segregation could be derived²⁷⁻²⁹. However, these techniques were time consuming, difficult and tedious and since the arrival and spreading of AES they are no more used.

In many cases, segregation can be described by a simple equation, the Langmuir-McLean isotherm (Figure 1d-f), describing segregation to a limited number of sites which leads to a maximum coverage Γ_A^{sat} when all sites are occupied, and with a free energy ΔG_A which is independent of coverage.

Then the degree of coverage

$$\Theta = \Gamma_A / \Gamma_A^{sat} \quad (3)$$

is given by

$$\Theta_A / (1 - \Theta_A) = x_A \exp (-\Delta G_A / RT) \quad (4)$$

Since $\Delta G_A = \Delta H_A - T \Delta S_A$ (5)

this leads to the form of the Langmuir-McLean equation

$$\ln \frac{\Theta_A}{1 - \Theta_A} = -\frac{\Delta H_A}{RT} + \frac{\Delta S_A}{R} + \ln x_A \quad (6)$$

which is used to derive the enthalpy and entropy of segregation from measurements of Θ_A at a constant bulk concentration x_A of the segregating species in dependence on temperature. Such measurements have been conducted, e.g. for the surface segregation of C, Si, N, P and S on iron and also for the grain boundary segregation of P, Sb and Sn (see Figure 6 and 8). The surface analyses were conducted by AES, observing the concentrations in situ on single or polycrystalline surfaces in dependence on temperature³⁰⁻⁴⁰.

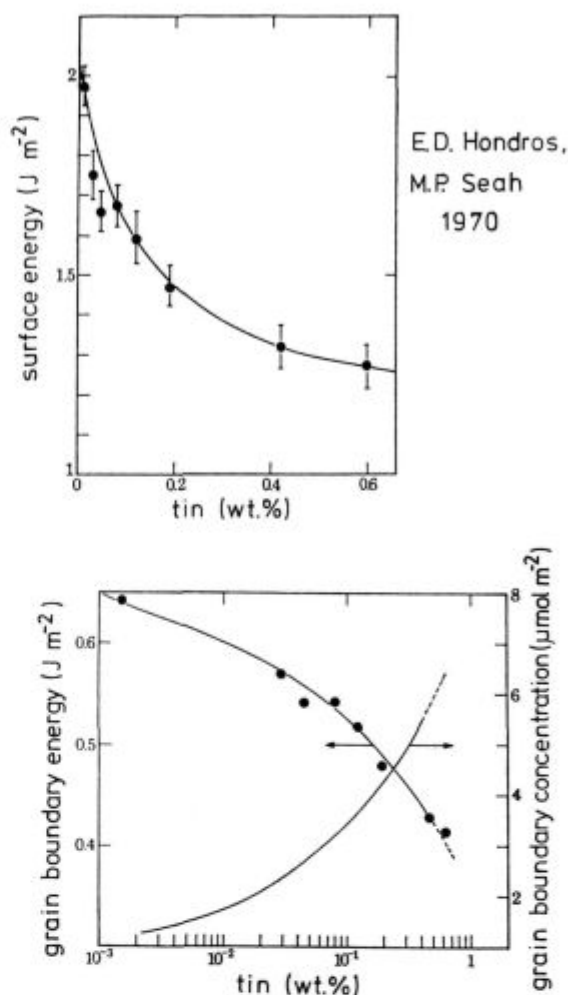


Figure 2: a) Surface energy and b) grain boundary energy of iron-tin alloys at 1420°C plotted as a function of the bulk tin content^{28,29} in (b) also the grain boundary segregation isotherm is given, which can be derived from the measurements

Slika 2: a) površinska energija in b) energija kristalnih mej zlitine železo-kositra pri 1420°C kot funkcija vsebnosti kositra v osnovni zlitini^{28,29} (b) podana je tudi izoterma segregacije po mejah zrn, ki jo lahko izračunamo iz meritev

The grain boundary analyses are also performed by AES, but after annealing the specimens for sufficient time at elevated temperature, then introducing them into the UHV system and fracturing in-situ by impact or tensile test^{35,36,39,40}. The analysis of intergranular fracture facets yields the grain boundary concentration, assuming that the content of impurity A has been distributed equally to both sides upon fracture.

The sites and structures attained in surface segregation can be elucidated using LEED (=low energy electron diffraction). In most cases the elements A are enriched on Fe(100) up to half a monolayer, corresponding to a c(2x2) structure, only for oxygen a complete monolayer and p(1x1) structure is attained. At grain boundaries rather high coverages are possible, for P in ferrite coverages nearly up to one monolayer have been observed. The observation of the LEED structures on single

crystal surfaces gives a good possibility for calibrating the AES measurements, also at grain boundaries, since the coverage for the saturated LEED structures is known.

Further information on segregated species can be obtained using photoelectron spectroscopy (XPS), the photolines obtained can indicate the ionization state of ions and the charge transfer between substrate and segregated atom⁴¹⁻⁴⁵. Generally, there is a transfer of negative charge (electrons) to the segregated atoms, which means that these (C, N, S, O, P etc.) are present as negatively charged atoms (anions) on the metal surface. This most probably is also the case in the grain boundary segregation, and it is supposed that such charge transfer weakens the cohesion of grain boundaries^{46,47} - leading to temper embrittlement of steels.

In the case that two elements are segregating simultaneously to a surface or a grain boundary, there is generally a competition for the sites available and the relative amount of both species in the surface depends on their free energy of segregation and concentrations in the bulk. Cases of competitive segregation have been studied on the iron surface for carbon and silicon³⁸, and at grain boundaries: carbon-phosphorus³⁶, carbon-sulfur⁴⁸, nitrogen-phosphorus³⁷... The simple formalism for competitive segregation without further energetic interaction of the segregating species is given by

$$\Theta_A / (1 - \Theta_A - \Theta_B) = x_A \cdot \exp(-\Delta G_A / RT) \quad (7)$$

$$\Theta_B / (1 - \Theta_A - \Theta_B) = x_B \cdot \exp(-\Delta G_B / RT) \quad (8)$$

which could be applied in the cases mentioned above. In the literature on temper embrittlement there is a lot of fuss about 'cosegregation', the mutually enhanced segregation of two species where attractive energetic interaction is to be assumed. In some cases the enhanced segregation can be explained in a different way - in other cases which are important here (Ni-Sn, Ni-Sb) formation of two- or three-dimensional phases at the grain boundaries may be suspected (see below, chapters 2.2 and 3.4).

1.3 Systems Fe-Sn and Fe-Sb

The solid solutions of Sn in α -Fe were determined by lattice parameter measurements^{49,50}. Accordingly, the solubility ranges from a maximum at 9,2 at% (17,7 wt%) at 900°C to 3,2 at% (6,56 wt%) at 600°C. The solubility limit in γ -Fe has been determined^{24,26} the γ -loop extends to 0,92 at% (1,93 wt%). Own investigations on Fe-0,054 wt% Sn and Fe-0,080 wt% Sn [unpublished], however, showed precipitation of Sn-rich particles on the grain boundaries after long-term annealing at 550°C; accordingly, there are uncertainties on the solubility at temperatures <600°C.

The solubility of Sb in α -Fe has been determined by several authors, the results are in substantial agreement⁴⁹. The solubility at 900°C is 4,19 at% Sb (8,71

wt%) decreasing at 600°C to 2,58 at% (5,46 wt%). The γ -loop extends till 1,1 at% Sb (2,36 wt%).

Experimental and theoretical studies have been conducted on the effects of other alloying elements on the antimony solubility, they were found to be the largest for M = Ti, Mn and Ni and small for M = Cr, Co. The presence of Ni e.g. reduces the solubility strongly, the phase precipitating is a hexagonal NiAs type: Fe₉₆Sb₂Ni₂. A cubic CaFe₂ type Fe₉₇Sb₂Ti is formed with Ti, which reduces the solubility at 900°C to 1,91 at%⁵². Strong interaction of Ni and Sb is also observed in surface segregation⁵³.

2 Interfacial segregation of Sn and Sb on and in iron and steels

2.1 Surface segregation of Sn and Sb on iron

The surface segregation of tin on Fe-Sn single crystals has been studied in the temperature range 450°C to 650°C, mainly on crystals with relatively high Sn concentrations so that always saturation coverages were observed, no dependence of coverage on temperature, so that the segregation enthalpy was not obtained^{54,55}. Each of the low index orientations exhibits a characteristic behaviour of the segregating Sn, the coverages attained are governed by segregation kinetics (**Figure 3a**). After heating the specimen for a short time a c(2x2) structure is observed, corresponding to half a monolayer coverage. But the segregation continues which leads to an order-disorder transition and a coverage somewhat higher than a monolayer (corresponding to $1,4 \cdot 10^{15}$ atoms Sn/cm²). The transition is accompanied by a shift of the photolines observed by XPS to values closely corresponding to the values characteristic for pure elemental tin, **Figure 3b**. Most probably the transition can be explained by formation of a two-dimensional nearly close packed layer of tin on Fe(100) with a high surface mobility. This segregation behaviour is different from the segregation in most systems Fe-A (A = C, N, S, P, Sb...) which always leads to a saturation at a surface coverage of 0,5. The driving force for the segregation of tin to higher coverages is probably the strong decrease of surface energy by the presence of a layer of tin. This layer at high coverage has properties similar to a layer of pure molten tin on iron, as indicated by the results of the XPS measurements. The segregation behaviour on Fe-Sn(111) is similar, there is an inflection point in the kinetics when the p(1x1) structure with one monolayer coverage is reached, which corresponds to $7 \cdot 10^{14}$ atoms Sn/cm² on Fe(111). After this surface structure is reached, further Sn segregation occurs, an order-disorder transition is observed and a Sn monolayer is attained. The segregation behaviour is different on Fe-Sn(110), here no intermediate adsorption structures were observed, but only structures with high Sn content, firstly a hexagonal structure corresponding to one monolayer of grey tin. Upon fur-

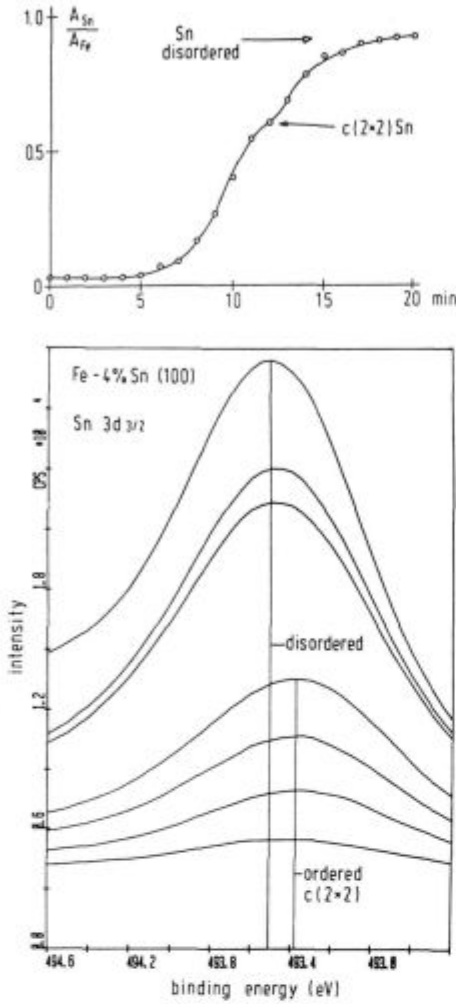


Figure 3: a) Kinetics of the tin surface segregation on Fe-4 wt% Sn(100) during heating to 650°C⁵⁴, at the inflection point indicated the structural phase transition from the ordered monolayer $c(2 \times 2)Sn$ to the disordered multilayer occurs; b) photolines observed during increasing surface concentration demonstrating the shift caused by the transition. **Slika 3:** a) Kinetika površinske segregacije na zlitini Fe-4 ut.% Sn(100) med žarjenjem do 650°C⁵⁴, prevoj označuje strukturni fazni prehod iz urejene monoplasti $c(2 \times 2)Sn$ v neurejeno večplastnost; b) fotolinije med naraščanjem površinske koncentracije prikazujejo kemijski premik, nastal zaradi prehoda

ther segregation a structure is formed which corresponds to a layer of the intermetallic compound FeSn of one unit cell thickness, **Figure 4a**.

The segregation behaviour of Sb on Fe-4 wt% Sb^{55,56} is similar on the orientations (100) and (111) to the behaviour of tin, on both orientations on ordered adsorption structure is formed, $c(2 \times 2)$ on (100), see **Figure 5**, and $p(1 \times 1)$ on (111) but upon continued segregation no elevated Sb surface concentration were observed, in contrast to Sn. On Fe(110) the presence of Sb caused faceting, the LEED patterns indicated formation of (111) and (111) planes, **Figure 4b**. Accordingly, the segregation enthalpy of Sb to Fe(111) must be very exothermic (negative), due to a strong decrease of the surface energy of Fe(111) which compensates the increase of total surface area by the faceting.

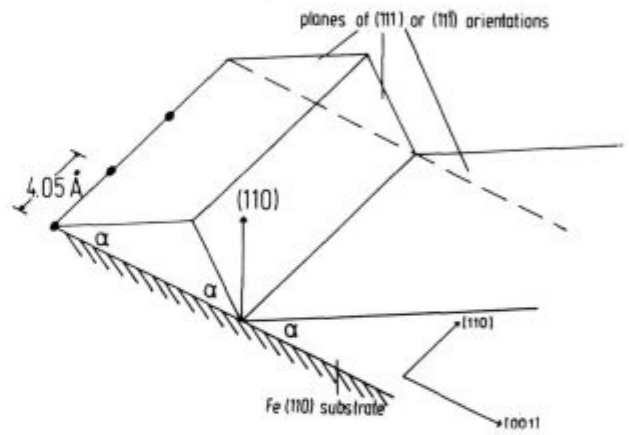
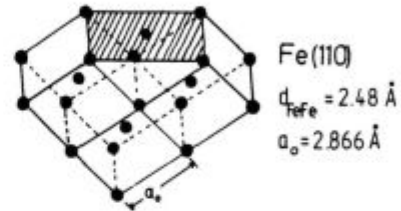
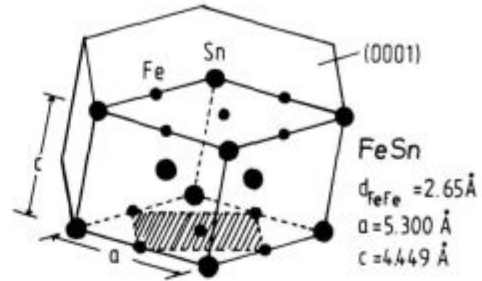


Figure 4: Phenomena on the Fe(110) face caused by segregation of Sn or Sb;

a) Supposed structure of the surface compound 'FeSn' formed by epitaxial stabilization on Fe-Sn(110) as the final saturation structure⁵⁴;

b) Faceting on Fe-Sb(110) under formation of (111) faces due to Sb segregation⁵⁶

Slika 4: Pojav na Fe(110) ploskvi, ki ga je povzročila segregacija Sn ali Sb;

a) predpostavljena struktura zlitine na površini 'FeSn', ki je nastala z epitaksialno stabilizacijo na Fe-Sn(110) kot končna nasičena struktura⁵⁴;

b) facetiranje na površini monokristala Fe-Sb(110), zaradi segregacije Sb se tvori (111) in (111) ploskvi

Three possibilities are demonstrated in the systems Fe-Sn and Fe-Sb for the behaviour upon segregation, (i) formation of adsorption structures such as $c(2 \times 2)$ or $p(1 \times 1)$, (ii) formation of surface phases such as two-dimensional grey tin and two-dimensional FeSn, or (iii) formation of facets to attain surface energies.

2.2 Grain boundary segregation of Sn and Sb

A fundamental study on grain boundary segregation in Fe-Sn alloys has been conducted after annealing in the temperature range 500-750°C for up to 5000 h³⁹. The results of the grain boundary analyses show a wide scatter

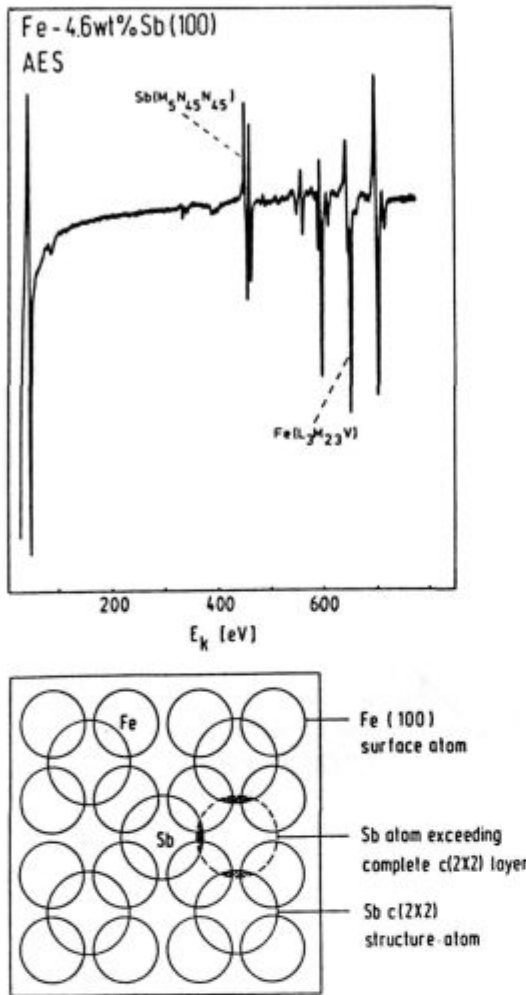


Figure 5: Surface segregation of Sb on Fe-Sb (100)⁵⁶; a) Auger spectrum after segregation at 640°C, corresponding to surface segregation; b) model for the Fe-Sb (100) c(2x2) structure derived from LEED study of the saturated surface

Slika 5: Površinska segregacija Sb na monokristalu Fe-Sb orientacije (100)⁵⁶; a) AES spekter posnet po segregaciji Sb pri 640°C; b) model za Fe-Sb (100) c(2x2) strukturo dobljen z metodo LEED na nasičeni površini

(**Figure 6a**) which may be caused by the strong dependence of tin segregation on grain boundary orientation. All data have been obtained for Sn concentrations within the α -solid solution range, no precipitates of intermetallic compounds should have formed. The tin concentrations are always below a monolayer, in contrast to the surface segregation behaviour. In spite of the large scatter the data were evaluated according to the Langmuir-McLean equation (**Figure 6b**), yielding the values for segregation enthalpy and entropy

$$\Delta H = -22,5 \text{ kJ/mol} \quad \Delta S = 26 \text{ J/mol K}$$

for 550°C results in good agreement with previous results of E. D. Hondros and M. P. Seah^{28,29}.

The enthalpy value is relatively low (P: $\Delta H = -34,3 \text{ kJ/mol}$ ^{35,36}), this indicates the rather low tendency for grain boundary segregation of Sn! Furthermore, due to

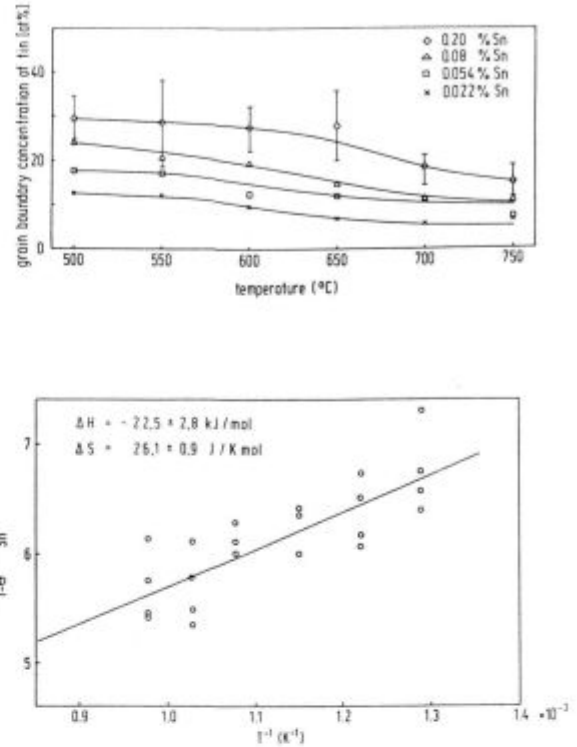
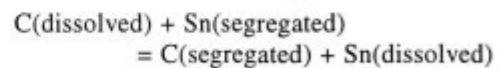


Figure 6: a) Grain boundary concentrations of tin in Fe-Sn alloys after annealing at elevated temperatures, measured by AES on intergranular fracture faces³⁹; b) evaluation of the measurements in (a) applying the Langmuir-McLean equation (6)

Slika 6: a) Koncentracija kositra v segregirani plasti na mejah zrn po žarjenju pri povišanih temperaturah, merjeno z metodo AES na interkristalnih prelomnih ploskvah³⁹; b) ovrednotenje meritev (a) z uporabo Langmuir-McLean enačbe (6)

its low segregation enthalpy Sn is kept from the grain boundaries effectively by the presence of carbon such as in plain carbon steels (**Figure 7**). As described in the introduction, an equilibrium of site competition between Sn and C occurs according to



In the presence of some ppm dissolved carbon, the tin is effectively removed from the grain boundaries.

However, in low alloy steels the concentration of dissolved C is reduced due to the formation of less soluble carbides with Cr and Mn. Tin segregation is possible if not Sn is displaced from the grain boundaries by segregated phosphorus. For rotor steels, CrMoV steels it is even dangerous to have too low phosphorus contents, since in application at high temperature if Sn segregation prevails, this easily leads to formation of creep cavities, due to the strong tendency for surface segregation of tin. The surface segregation of Sn decreases the surface energy of pores and cavities, stabilizes such defects and accelerates their growth (see chapter 3.2).

In must be kept in mind that the data given above are average values and have an integral character, since the grain boundary segregation of tin in iron is strongly de-

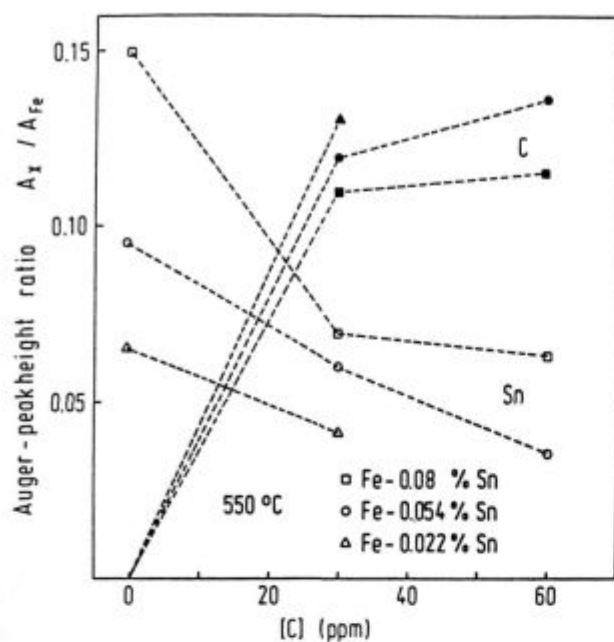


Figure 7: Grain boundary segregation of Sn and C in Fe-Sn-C alloys in dependence on the bulk carbon concentration after equilibration at 550°C, demonstrating the displacing effect of carbon on segregated Sn³⁹

Slika 7: Segregacija Sn in C po mejah zrn v Fe-Sn-C zlitinah v odvisnosti od koncentracije ogljika v osnovnem materialu pri ravnotežju pri 550°C

pendent on the misorientation, increasing with the tilt angle of misorientation between the grains⁵⁷. Sn causes grain boundary hardening, excess hardness extending to many microns on either side of the grain boundary, also increasing with the misorientation. This is a well documented effect but not well understood^{57,58}.

For temper embrittled Ni-Cr steels there are strong indications that Sn is present at the grain boundaries coupled with Ni in an bidimensional phase corresponding to an intermetallic compound such as Ni₃Sn₂, this has been concluded from Mössbauer spectroscopy and TEM work⁵⁹⁻⁶¹.

The grain boundary segregation of Sb was investigated for Fe-Sb and Fe-Sb-C alloys after equilibration at temperatures between 550°C for sufficient time^{62,63}. The analysis of intergranular fracture faces by AES calibrated on the base of the surface segregation studies shows relatively low interfacial concentrations, see **Figure 8**, and a wide scatter of results. The plot of the data according to the Langmuir-McLean equation leads to the values for segregation enthalpy and entropy:

$$\Delta H = -19 \text{ kJ/mol} \quad \Delta S = 28 \text{ J/mol K}$$

Thus, the segregation enthalpy is even lower than for Sn, which emphasizes the low tendency for grain boundary segregation of Sb. However, even small grain boundary concentrations of Sb cause marked grain boundary embrittlement and prevailing intergranular fracture. Also the segregant Sb is effectively displaced from grain

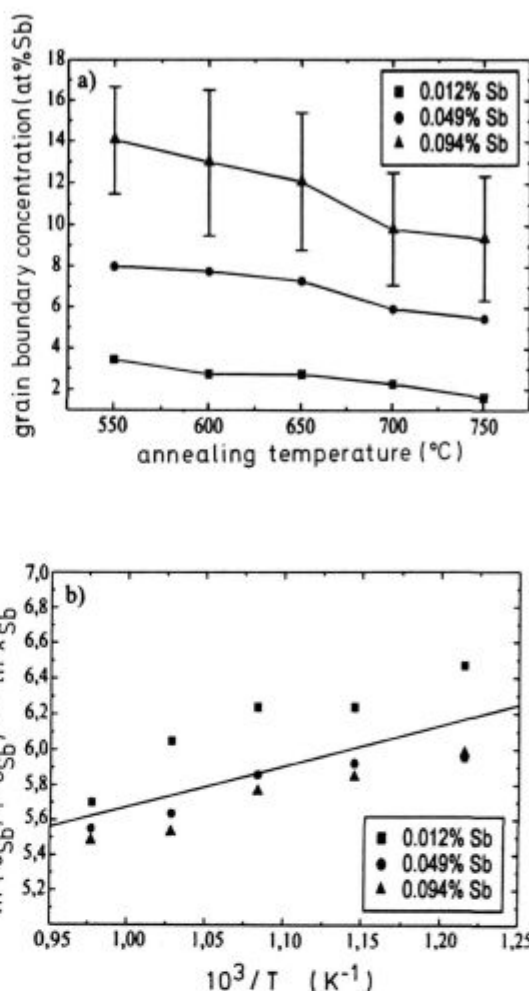


Figure 8: a) Grain boundary concentrations of Sb in Fe-Sb alloys, plotted vs equilibration temperature⁶²; b) plot of the data in (a) according to the Langmuir-McLean equation (6)

Slika 8: a) Segregacija Sb po mejah zrn v Fe-Sb zlitini v odvisnosti od ravnotežne temperature⁶²; b) prikaz podatkov v (a), ki ustrezajo Langmuir-McLean enačbi (6)

boundaries by carbon, small concentrations of dissolved carbon < 60 wtppm can shift the displacement equilibrium to low Sb segregation and also lead to a marked reduction of intergranular fracture, see **Figure 9**⁶⁴. Carbon not only removes Sb from the grain boundaries, but also enhances the grain boundary cohesion and enforces transgranular fracture. The effect of carbon also was demonstrated by notch-impact tests on Fe-Sb-C alloys, see **Figure 10**. As in the case of Sn, for unalloyed carbon steels the danger of embrittlement by Sb is minor, there will be always enough dissolved and segregated carbon to avoid Sb grain boundary segregation. Only for alloyed steels, in which the carbon is tied up by carbide forming elements, Cr, Mn, etc., embrittlement is possible during heat treatment or use of steels in an elevated temperature range.

Several authors have claimed an effect of nickel, enhancing the grain boundary segregation of Sb, however, this effect could not be reproduced in recent studies on

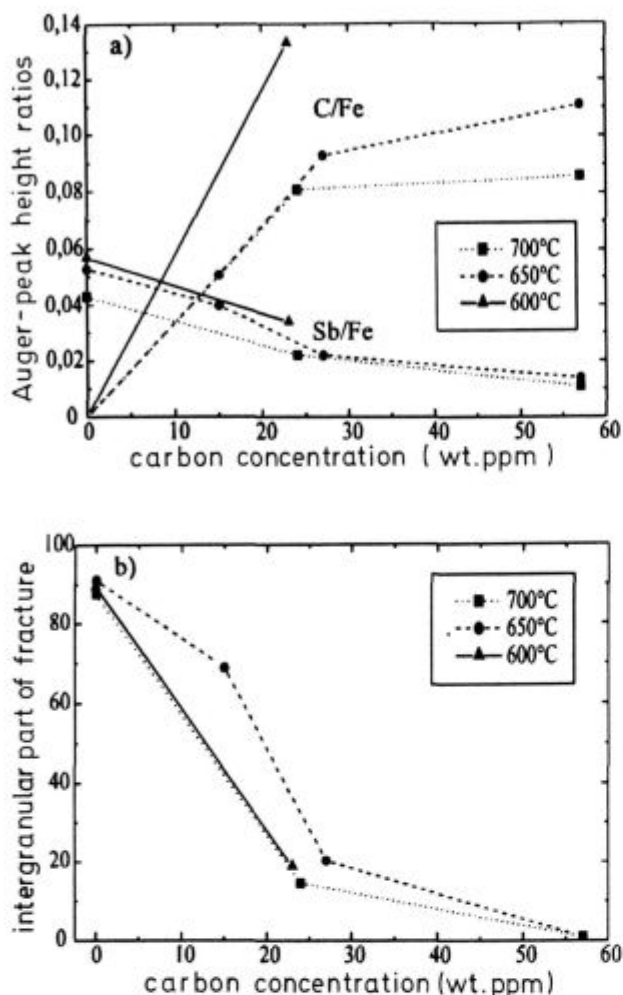


Figure 9: a) Grain boundary segregation of Sb and C in Fe-Sb-C alloys after equilibration at different temperatures, plotted in dependence on the bulk concentration, demonstrating the displacing effect of carbon on segregated Sb^{62,63}; b) intergranular part of fracture in dependence on bulk carbon concentration

Slika 9: a) Ravnotežna koncentracija Sb v segregirani plasti na mejah zrn v zlitini Fe-Sb-C pri različnih temperaturah, prikazana v odvisnosti od koncentracije C v osnovnem materialu, prikazuje pojav ko ogljik izrine Sb v segregirani plasti^{62,63}; b) interkristalna ploskev preloma v odvisnosti od koncentracije ogljika v osnovnem materialu

Fe-Ni-Sb alloys⁶⁴. In earlier studies^{65,66} of Fe-Sb and Fe-Ni-Sb alloys at 560°C an increase of Sb segregation was observed with hte Ni-content and Ni also segregates to the grain boundaries, its segregation being only slightly affected by the presence of Sb. For low alloy Ni-Cr steels the authors^{65,66} conclude that the Sb-segregation is a complex function of the total alloy composition. When Mn is present in these steels it causes precipitation of an antimonide and greatly reduces Sb-segregation. A detailed investigation of a 3,5 Ni-1Cr-steel after embrittlement at 480°C demonstrates a dependence on the microstructure⁶⁷. Intergranular embrittlement in a quenched and tempered martensitic microstructure was associated with the segregation of phosphorus, which is possible since the carbon activity is reduced by precipitation of

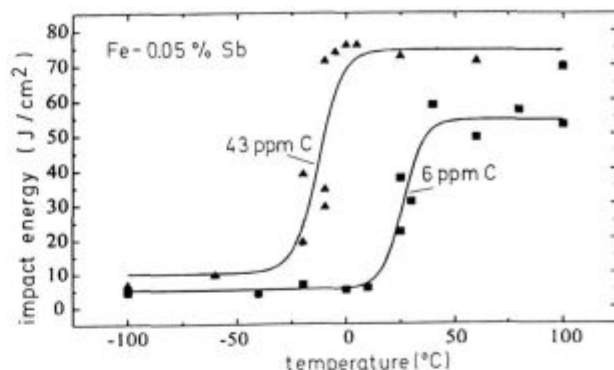


Figure 10: Results of notch impact tests on an Fe-Sb alloy with different carbon concentrations⁶³. The ductile-brittle transition temperature is shifted to lower temperatures by carbon, due to the removal of Sb from the grain boundaries and increase of grain boundary cohesion by segregated carbon

Slika 10: Rezultati udarnih preizkusov na zlitini Fe-Sb z različnimi vsebnostmi ogljika⁶³. Temperatura prehoda duktilno-krhko je premaknjena k nižjim temperaturam zaradi ogljika, le-ta izpodrine Sb z mej zrn in poviša kohezijo

chromium rich carbides at the grain boundaries. the embrittlement in the bainitic microstructure was associated with the segregation of antimony, since the carbon activity is relatively high due to the formation of cementite type carbides. Prolonged embrittlement of the bainite produced a low energy fracture. Increased nickel and antimony concentrations at the grain boundaries were associated with the formation of a fine grain boundary precipitate. The increased carbon activity continued to prevent appreciable P segregation but could not inhibit the 'cosegregation' of Ni and Sb⁶⁷.

2.3 Segregation of Sb and Sn at internal interfaces

Sb can be trapped by TiC precipitates in Fe. A dense dispersion of TiC, produced by ion implantation and annealing at 600-700°C, ties up Sb effectively⁶⁸. Continued annealing leads to slow release of Sb into the matrix in a diffusion and trapping process. The Sb is present at the interface TiC/ferrite, and not in the TiC, the binding enthalpy is -35,6 kJ/mol⁶⁸⁻⁷⁰. This interfacial segregation may provide a means for keeping Sb from grain boundaries in ferritic steels to suppress embrittlement. Similar trapping has been observed at TaC and Cu precipitates in Fe at 600°C⁷¹.

Trapping or segregation of Sn at MnS particles has been observed in Fe-3% Si doped with tin. The Sn was clearly enriched compared to the grain boundaries, this segregation retards the growth rate of the MnS particles so that in Sn doped alloy they are much smaller than in Sn-free Fe-3% Si⁷². The size of the precipitates affects the primary and secondary recrystallization, thus influencing the magnetic properties of Si steels, see chapter 3.1.

In the eutectoid transformation of austenite to cast iron, minor additions of Sb (0,08 wt%) or Sn (0,12 wt%)

were found to inhibit the $\gamma \rightarrow \alpha + \text{graphite}$ and the $\text{Fe}_3\text{C} \rightarrow \alpha + \text{graphite}$ reaction paths, but did not significantly affect the metastable $\gamma \rightarrow \alpha + \text{Fe}_3\text{C}$ reaction⁷³. Scanning Auger microprobe analysis indicated that Sn and Sb adsorb at the graphite/metal interface. The segregated layer acts as a barrier for the access of carbon to the graphite nodules. With the graphite disabled as a sink for carbon, the metal transforms as a nongraphite steel.

3 Effects of interfacial segregation of Sn and Sb on steel properties

3.1 Effects of surface segregation on the texture of electrical sheet

A (100) [001] texture of Fe-Si can be achieved with the aid of adsorption or segregation of different species: O, S, Sb, Sn etc. The (100) [001] texture cannot compete losswise with the (110) [001] texture if unidirectional magnetization is important. In applications where the magnetization must occur in all directions in the plane of the sheet such as in motors or generators the (100) [001] texture is favourable since the plane of the sheet does not contain the hard (111) direction of magnetization, but even in transformers lower losses can be obtained by using some (100) [001] texture. After the primary recrystallization, the growth of grains is governed by the surface energy, preferential growth of grains with a low surface energy occurs in the secondary recrystallization. In absence of oxygen or other adsorbing or segregating species γ_{110} is the lowest surface energy and (110) [001] grains grow. When sufficient oxygen or sulfur is present γ_{110} and (100) grains become stable in the surface⁷⁴⁻⁷⁶, see also **Figure 1**.

Presence of oxygen and sulfur is not well possible in the production process of non-oriented electrical sheet. The annealing for secondary recrystallization is done in dry hydrogen at about 900°C. Presence of sulfur would cause precipitation of MnS particles in the steels which may hinder the reorientation of the magnetic domains. Thus, other elements such as Sn and Sb were successfully used as alloying additions to improve the texture and magnetic properties of non-oriented steel sheet^{77,78}. The alloying additions may not be too high to obtain the wanted (100) [001] texture, for too high activities and surface coverages the surface energies of nearly all orientations are decreased so strongly that no preferential growth of (100) is attained. Sb has proved to have another advantageous effect, it suppresses widely the internal oxidation of the alloying elements Si, Al and Mn which is possible during the decarburization treatment and causes increasing permeability deterioration with increasing subscale depth⁷⁹. Also in the production of high induction and high permeability grain oriented Fe-Si, the presence of Sb and Sn can have positive effects, yielding a more precise (110) [001] secondary recrystallization

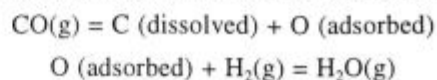
texture than in conventional Fe-Si. In earlier work it was assumed that Sb and Sn are effective on the primary recrystallization, retarding primary grain growth in cooperation with BN and S, less S being necessary than without Sb and Sn. But in recent studies it was found that grain boundary segregation of Sb and Sn is negligibly low in the silicon steel sheet after the usual thermal treatment. Obviously, the effect of Sb and Sn is caused by the surface segregation during recrystallization annealing. The surface segregation decreases the surface energy of grains with (100) orientation in the plane of the steel sheet and the grains with low surface energy grow on account of grains with other space orientation in the sheet plane. The role of the surface segregation has been confirmed by extended studies on silicon steel doped with Sb and Sn¹²⁻²⁰. Only a controlled surface segregation promotes the wanted selective grain growth. For too high Sb and Sn concentrations the surface energy of all orientations are strongly decreased and no preferential growth of (100) is obtained. For steels with a high Sb content rather the unwanted growth of (111) is to be expected, since the surface concentration on that plane is highest⁵⁶. Furthermore, it has been stated that Sb and Sn retard the decarburization⁷⁹, which is also a very important process in the production of electrical steel sheet - so this again would be a negative effect of Sb and Sn surface segregation.

3.2 Effect of surface segregation in creep of steels

Due to their strong tendency to surface segregation Sn and Sb can very negatively affect the creep behaviour of heat resistant CrMo- and CrMoV- steels used for turbine rotors and blades⁸⁰. The failure of such steels occurs by formation of creep cavities at the grain boundaries and in the steel matrix and the coalescence of the cavities to cracks. The nucleation of the cavities mostly starts at inclusions, such as sulfides (MnS) and oxides⁸¹. But the nucleation is favoured and accelerated by the presence of Sn or Sb which will immediately segregate to the free metal surface of a pore forming at an inclusion or at a grain boundary. The segregation decreases the surface energy, the pores are stabilized and can grow to cavities under further surface segregation. This effect of Sn has been observed for a CrMoV- steel^{39,40} measuring creep curves for melts doped with different Sn-concentrations. The higher the Sn content of the steel the earlier they failed by rupture in the creep test, **Figure 11**.

3.3 Effects on the carburization of case hardening steels

Surface segregation on Sn and Sb can effectively retard the carburization of case hardening steels⁸². The carburization is generally conducted at about 930°C in CO-H₂-H₂O atmospheres. In the beginning its rate is controlled mainly by the surface reaction sequence



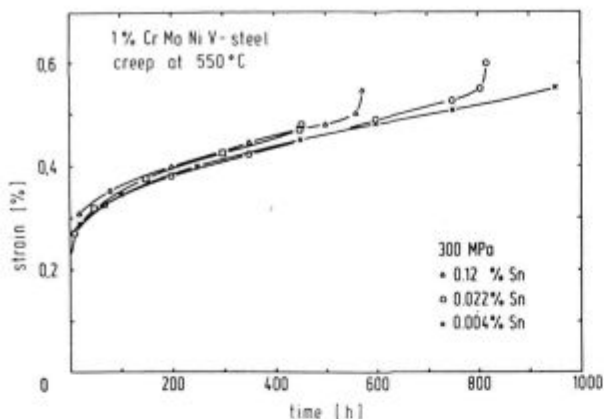


Figure 11: Creep curves for 1% CrMoNiV- steel at 300 MPa and 500°C³⁹, effect of different Sn-contents - with increasing Sn-content the rupture time is markedly decreased
Slika 11: Krivulje lezenja za jeklo 1% CrMoNiV pri 300 MPa in 550°C³⁹, vpliv različnih vsebnosti Sn - z naraščajočo vsebnostjo Sn je prelomni čas opazno znižan

and later on a coupled surface reaction and diffusion control determines the rate of carburization. The surface reaction rate can be described by

$$r = \beta([C]_{eq} - [C]_s)$$

where $[C]_{eq}$ and $[C]_s$ are the equilibrium and the actual surface concentration of carbon and β is the carbon transfer coefficient, which contains dependencies on partial pressures and temperature⁸³. Extended thermogravimetric studies of carburization on steels doped with Sn, Sb, Cu, P or Pb demonstrated a strong effect of Sb on the coefficient β (see **Figure 12a**), whereas the effect of the other elements is much less. This retardation of carbon transfer is caused by the blocking of surface sites for reaction, the adsorption and dissociation of CO, by segregated Sb. The surface segregation of Sb and Sn on the case hardening steels was demonstrated by AES studies, after exposure in the carburization atmosphere at 900°C, see **Figure 12b**. Segregation in the UHV chamber leads to displacement of Sb and Sn by sulfur, however, in the carburization atmosphere the sulfur would be removed by the reaction $S(\text{absorbed}) + H_2(g) = H_2S(g)$. The presence of too high levels of Sb in case hardening steels would lead to too low carbon contents after the usual carburization period and insufficient hardening of the workpieces, see **Figure 12c**. Thus, a specification for Sb-content < 25 wt ppm was recommended for case hardening steels, whereas concentration of the other tramp elements may be in the usual range⁸⁴.

3.4 Temper embrittlement

Reversible temper embrittlement occurs upon slowly cooling of steels through the temperature range 550 to 350°C after annealing (tempering) at higher temperatures or during application of steels in this range. Temper em-

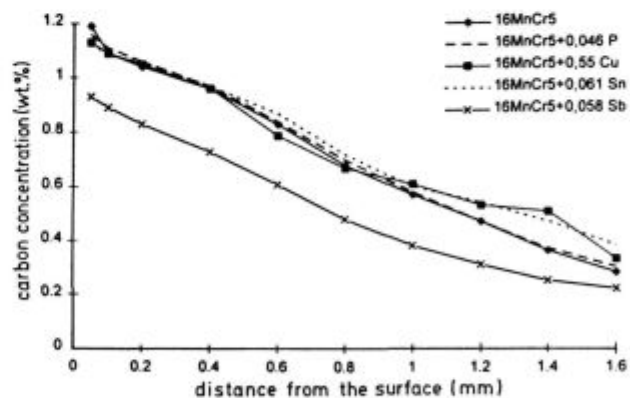
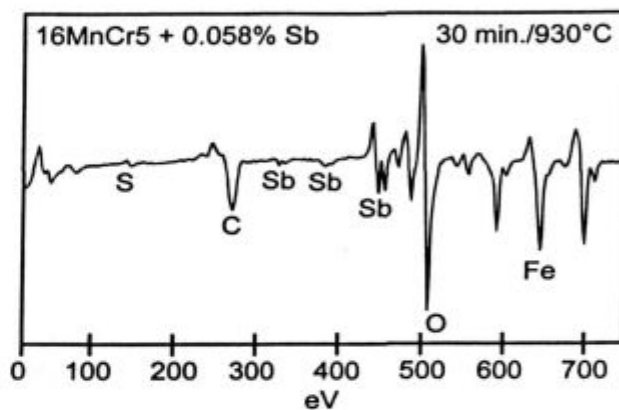
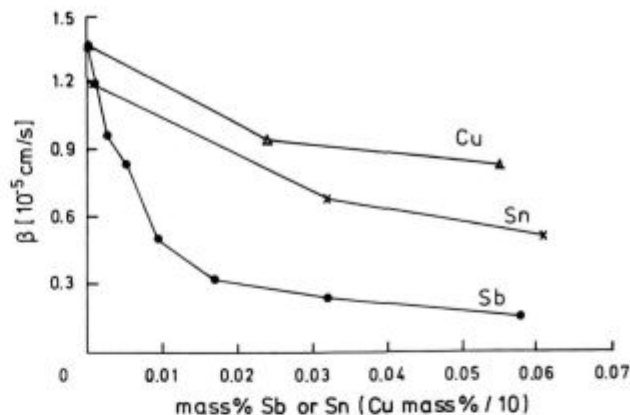


Figure 12: Effects of Sb, Sn and Cu on the gas carburization of a case-hardening steel at 930°C^{82,84}, a) carbon transfer coefficient β in dependence on bulk concentrations of Sb, Sn or Cu, b) Auger spectrum of the Sb-doped steel after heating in hydrogen to 930°C, c) carbon concentration profiles after gas carburization of samples in an industrial furnace

Slika 12: Vpliv Sb, Sn in Cu na plinsko naogljčenje jekla za cementacijo pri 930°C^{82,84}, a) β prenosni koeficient ogljika v odvisnosti od koncentracije Sb, Sn ali Cu v osnovnem materialu, b) AES spekter jekla legiranega z Sb po žarjenju v vodiku pri 930°C, c) koncentracijski profil ogljika po plinskem naogljčevanju vzorcev v industrijski peči

embrittlement is caused by grain boundary segregation of P, Sn, Sb and As⁶¹⁻⁷² but severe embrittlement is observed only if the alloying elements Ni, Cr and Mn are present, such as in low alloy turbine steels. In earlier years this fact was explained by 'cosegregation', e.g. of Cr and P, however especially for this case it could be clearly shown that Cr alone has no enhancing effect on P-segregation^{35,36}. In fact, Cr and Mn decrease the carbon solubility in steels, and the effect of carbon on P-segregation, i.e. removal of P from the grain boundaries by displacement by C, is reduced in the presence of Cr and Mn, thereby allowing more P-segregation. 'Cosegregation' was also suspected for Ni and Sb, and Ni and Sn, but most probably the strong effect of these combinations on embrittlement are due to interfacial formation of intermetallic compounds of these elements. Steels without Ni do not show embrittlement by Sn or Sb⁸⁵⁻⁹⁶.

Temper embrittlement is a particular problem for low alloy steels, e.g. Ni-Cr-Mo-V rotor steels and Cr-Mo pressure vessels. Temper embrittlement does not occur in plain carbon steels with less than 0.5% Mn. At high Mn concentrations, however, P-segregation is possible in plain carbon steels and also a 'cosegregation' of Mn and Sb is supposed to occur. However, the effect of Mn can easily be explained by the reduction of carbon activity caused by formation of Mn-rich carbides⁹⁷. Thereby, carbon segregation is reduced which allows grain boundary segregation of P, Sn and Sb.

3.5 Hydrogen induced cracking

The threshold stress intensity for cracking of a Ni-Cr-Mo steel is strongly reduced by grain boundary segregation of Sb, Sn and P⁹⁸⁻¹⁰⁰. In the presence of hydrogen this threshold stress intensity is lowered further, but it is the impurity effect which is dominant, the hydrogen merely accentuates the tendency for brittleness already present.

It must be emphasized again that for embrittlement of steels by Sb the presence of Ni and Cr is necessary. Sb causes intergranular fracture in the constant strain rate test, it is five times more effective in inducing intergranular fracture at cathodic potentials than S, the results are consistent with H-permeation studies in Fe as affected by Sb and S^{101,102}.

3.6 Possible effects of grain boundary segregation in interstitial free steels

One may expect that grain boundary segregation of Sn and Sb is possible in interstitial free steels (i.f. steels). Such steels have very low concentrations of C and N in order to attain good deep drawing properties, and thus the tramp elements are not kept away from the grain boundaries by segregated carbon (see **Figure 10**). The effects of Sn and Sb in deep drawing steels were not studied as yet, but a behaviour similar to P^{103,104} may be expected. Brittle behaviour was found for steels with

very low C content (< 300 ppm), caused by P at grain boundaries. Some i.f. steels are alloyed with Ti to tie up the interstitial elements, but Ti is also effective in scavenging the phosphorus forming a very stable phosphide. Also TiC as a precipitate is able to trap phosphorus and to keep it from the grain boundaries to a certain extent, such trapping effect has also been reported for Sb at the TiC/ferrite interface⁶⁸⁻⁷⁰. Anyway, similar as P can be deleterious for the properties of certain deep drawing steels with low C and no TiC or excess Ti, also Sn and Sb may adversely affect the ductility of such steels. Especially if steels with high Sn and/or Sb contents are slowly cooled after batch annealing or coiling, they may segregate to grain boundaries and cause embrittlement. On the other hand, also positive effects may occur on the texture, as in the case of electrical steel sheet. Effects of Sb and Sn on the texture of deep-drawing steels are currently investigated¹⁰⁵.

4 Conclusions

Generally, tramp elements such as Sn and Sb can have effects on steel properties only if they enrich at interfaces, the enrichment by equilibrium segregation leads to coverages in the range of a monolayer depending on bulk concentration and decreases with temperature. Utilizing Auger-electron spectroscopy the thermodynamics of segregation to surfaces and grain boundaries can be elucidated.

The solubilities of Sn and Sb in the ferritic matrix are relatively high, the solubility is strongly decreased in the presence of some elements such as Ni which form intermetallic compounds with Sn and Sb.

The tendency for surface segregation of Sn and Sb is very high, as yet no thermodynamic data have been determined since always saturation was observed. The segregation coverages and structures are very different for different crystallographic orientations, therefore the decrease of surface energy will be strongly dependent on orientation and marked effects of Sn and Sb on the stability of different crystallographic planes are to be expected.

Sn and Sb segregate to grain boundaries in ferrite, the extent of segregation strongly depends of the misfit of the grains. The tendency for grain boundary segregation of Sn and Sb is relatively low, as indicated by the results on equilibrium segregation in binary alloys in the temperature range 500 to 750°C. This can also be seen from the segregation enthalpies: -22,5 kJ/mol Sn and -19 kJ/mol Sb.

Sn and Sb also segregate to interfaces, for Sb at interfaces ferrite/TiC and for Sn at the interface ferrite/MnS.

In the annealing of steel sheet the surface segregation of Sn and Sb affects the stability of certain orientations. For intermediate concentrations the (100) orientation appears to be stabilized, for higher contents the (111) orientation becomes stable. These effects are of importance

in the production of electrical Fe-Si steel sheet and may also be useful in the production of deep-drawing steels.

The strong tendency for surface segregation of Sn (and Sb) plays a role in the creep of heat resistant steels, since formation and growth of creep cavities is enhanced by surface segregation decreasing the surface energy of the cavities. This was demonstrated for Sn doped CrMoV-steels.

Surface segregation of Sn and Sb affects the carburization of case hardening steels. Especially Sb strongly retards the carbon transfer and may cause insufficient carburization.

Grain boundary segregation of Sn or Sb causes embrittlement. Temper embrittlement of low alloy steels only occurs in the presence of Ni and Cr. Obviously, reduction of carbon activity by Cr and formation of intermetallics Ni_xSn_y resp. Ni_xSb_y is necessary for temper embrittlement.

Hydrogen induced cracking can be favoured by Sn and Sb grain boundary segregation. However, as for temper embrittlement the presence of Ni and Cr appears to be a precondition of such effect of Sn and Sb.

In interstitial free steels one may expect strong effects of Sn and Sb since these elements are not kept away from the grain boundaries by carbon. Addition of Ti may scavenge Sn and Sb, either by direct interaction or by trapping effect of TiC.

5 References

¹ D. A. Melford: *Phil. Trans. Roy. Soc. London*, A295, 1980, 89
² M. Torkar, F. Vodopivec: *Železarski zbornik*, 15, 1981, 61
³ F. K. Peters, H. J. Engell: *Archiv Eisenhüttenwes.*, 30, 1959, 275
⁴ F. Vodopivec, A. Kohn, J. Benard: *Comptes Rendus A. S.*, 255, 1962, July, 296-298
⁵ F. Vodopivec: *Métaux-Corrosion-Industries*, 452, 1963, April, 159-170
⁶ F. Vodopivec, A. Kohn: *Comptes Rendus A. S.*, 253, 1963, July, 448-450
⁷ F. Vodopivec, A. Kohn, J. Philibert, J. Manenc: *Mem. Scient. Rev. de Métallurgie*, 60, 1963, 11, 808-818
⁸ F. Vodopivec, L. Kosec: *Comptes Rendus A. S.*, 262, 1966, April, 1124-1127
⁹ F. Vodopivec, L. Kosec: *Archiv Eisenhüttenwes.*, 40, 1969, 2, 118-121
¹⁰ L. Kosec, F. Vodopivec, R. Tixier: *Métaux-Corrosion- Industries*, 1969, May-525, 1-17
¹¹ F. Vodopivec, L. Kosec: *Radex-Rundschau*, 8, 1969, 4, 639-649
¹² F. Vodopivec, F. Marinšek, F. Grešovnik, D. Gnidovec, M. Praček, M. Jenko: *Journal of Magnetism and Magnetic Materials*: 97, 1991, 281-285
¹³ F. Vodopivec, M. Jenko, F. Marinšek, F. Grešovnik: *Vacuum*, 43, 1992, 497-500
¹⁴ M. Jenko, F. Vodopivec, B. Praček: *Vacuum*, 43, 1992, 449-451
¹⁵ M. Jenko, F. Vodopivec, B. Praček: *Appl. Surface Science*, 1993, 70/71, 118
¹⁶ M. Jenko, F. Vodopivec, B. Praček, M. Godec, D. Steiner: *Journal of Magnetism and Magnetic Materials*: 133, 1994, 229-232
¹⁷ M. Jenko, F. Vodopivec, H. J. Grabke, H. Viehhaus, B. Praček, M. Lucas, M. Godec: *Steel Research*, 65, 1994, 500-504
¹⁸ M. Jenko, F. Vodopivec, H. Viehhaus, M. Milun, T. Valla, M. Godec, D. Steiner-Petrovič: *Fizika*, A4, 1995, 3, 91-98
¹⁹ M. Jenko, F. Vodopivec, H. J. Grabke, H. Viehhaus, M. Godec, D. Steiner-Petrovič: *Journal de Physique IV*, Colloque C7, 5, 1995, C7-225-231
²⁰ R. Mast, H. J. Grabke, M. Jenko, M. Lucas: *Materials Sci. Forum*, 207-209, 1996, 401

²¹ E. Hondros, M. P. Seah: *Int. Metals Review*, 222, 1977, 262
²² C. L. Briant, S. K. Banerji: *Int. Materials Reviews*, 232, 1978, 164
²³ C. L. Briant, H. J. Grabke: *Mat. Sci. Forum*, 46, 1989, 253
²⁴ H. J. Grabke: *J. Iron Steel Inst. Japan Int.*, 29, 1989, 529-538
²⁵ H. J. Grabke: Grain Boundary Segregation of Impurities in Iron and Steels and Effects on Steel Properties, in *Impurities in Engineering Materials*, Ed. C. L. Briant, M. Dekker, in press
²⁶ W. B. Pearson: *A Handbook of Lattice Spacings and Structures of Metals and Alloys*, Pergamon Press, London, issued as N.R.C. No. 4303
²⁷ E. D. Hondros, M. P. Seah: *Proc. Roy. Soc. London*, A 286, 1965, 479
²⁸ M. P. Seah, E. D. Hondros: *Proc. Roy. Soc. London*, A 335, 1973, 191
²⁹ E. D. Hondros, M. P. Seah: *Met. Trans.*, 8A, 1977, 1363
³⁰ H. J. Grabke, G. Tauber, H. Viehhaus: *Scr. Metall.*, 9, 1975, 1181
³¹ H. J. Grabke, W. Paulitschke, G. Tauber, H. Viehhaus: *Surf. Sci.*, 63, 1977, 377
³² H. J. Grabke, H. Viehhaus, G. Tauber: *Archiv Eisenhüttenwes.*, 49, 1978, 391
³³ H. J. Grabke: *Mater. Sci. Eng.*, 42, 1980, 91
³⁴ H. Viehhaus, H. J. Grabke: *Surf. Sci.*, 109, 1981, 1
³⁵ H. Erhart, H. J. Grabke: *Železarski zbornik*, 15, 1981, 33, Proceed. Int. Conf. 'Residuals in Iron and Steel', 1980 Ljubljana
³⁶ H. Erhart, H. J. Grabke: *Met. Sci.*, 15, 1981, 401
³⁷ H. Erhart, H. J. Grabke: *Scripta Met.*, 15, 1981, 531-534
³⁸ H. de Rugy, H. Viehhaus: *Surf. Sci.*, 173, 1986, 418
³⁹ W. Jäger, H. J. Grabke, R. Möller: *Proc. Int. Conf. on 'Residuals and Trace Elements in Iron and Steel'*, Portorož, Oct. 1985, ed. by F. Vodopivec, Inst. Metall., Ljubljana, 1986, 217-237
⁴⁰ W. Jäger, H. J. Grabke, Jin Yu: *Proc. 2nd Int. Conf. on Creep and Fracture of Engineering Materials and Structures*, ed. B. Wilshire, D. R. Owen, Pineridge Press, 1984, 649-659
⁴¹ B. Egert, G. Panzner: *Surface Sci.*, 118, 1982, 345-368
⁴² B. Egert, G. Panzner: *Physical Review B*, 28, 1983, 8
⁴³ G. Panzner, B. Egert: *Surface Sci.*, 144, 1984, 651-664
⁴⁴ G. Panzner, W. Diekmann: *Surface Sci.*, 160, 1985, 253-270
⁴⁵ W. Diekmann, G. Panzner, H. J. Grabke: *Surf. Interface Analysis*, 2, 1986, 184
⁴⁶ W. Losch: *Acta Metall.*, 27, 1979, 1885
⁴⁷ R. P. Messmer, C. L. Briant: *Acta Metall.*, 30, 1980, 457
⁴⁸ G. Tauber, H. J. Grabke: *Ber. Bunsenges. Physikal. Chemie*, 82, 1978, 298
⁴⁹ O. Kubaschewski: *Iron - Binary Phase Diagrams*, Springer Verlag, 1982
⁵⁰ M. Nageswararao, C. J. McMahon, Jr., H. Herman: *Met. Trans.*, 5, 1974, 1061
⁵¹ M. Arita, M. Ohyama, K. S. Goto, M. Someno: *Z. Metallkde.*, 72, 1981, 244
⁵² M. C. Cadeville, M. Maurer: *Mat. Sci. a. Engineering*, 51, 1981, 147
⁵³ Ph. Dumoulin, M. Guttman: *Mat. Sci. a. Engineering*, 42, 1980, 249
⁵⁴ H. Viehhaus, M. Rösenberg: *Surf. Sci.*, 159, 1985, 1
⁵⁵ M. Rösenberg, H. Viehhaus: *Ber. Bunsenges. Phys. Chem.*, 90, 1986, 301
⁵⁶ M. Rösenberg, H. Viehhaus: *Surf. Sci.*, 172, 1986, 615
⁵⁷ T. Watanabe, S. Kitamura, S. Karashima: *Acta Met.*, 28, 1980, 455
⁵⁸ M. Braunovic: *Canadian Metallurg. Quart.*, 13, 1974, 211
⁵⁹ J. M. Titchmarsh, B. C. Edwards, G. Gabe, B. L. Eyre: *Nature*, 278, 1979, 38
⁶⁰ B. C. Edwards, B. L. Eyre, T. E. Cranshaw: *Nature*, 269, 1977, 47
⁶¹ T. E. Cranshaw: *J. Physique*, Colloque C2, supplément No. 3, 40, 1979, C2-167
⁶² R. Mast, H. J. Grabke, M. Jenko, M. Lucas: *Materials Science Forum*, 207-209, 1996, 401-404
⁶³ R. Mast, H. Viehhaus, M. Lucas, H. J. Grabke: in *Nichtmetalle in Metallen 96*, ed. D. Hirschfeld, 51-60
⁶⁴ R. Mast, H. Viehhaus, M. Lucas, H. J. Grabke: *4th Conf. on Materials and Technology*, Oct. 1996, Portorož, Slovenia
⁶⁵ C. L. Briant, A. M. Ritter: *Acta Met.*, 32, 1984, 2031
⁶⁶ C. L. Briant: *Acta Met.*, 35, 1987, 149
⁶⁷ A. Wirth, I. Andreoni, G. Gregory: *Surface a. Interf. Anal.*, 9, 1986, 157
⁶⁸ S. M. Myers, D. M. Follstaedt, H. J. Rack: *Met. Trans.*, 11A, 1980, 1465
⁶⁹ J. A. Knapp, D. M. Follstaedt: *Appl. Phys. Lett.*, 37, 1980, 9, 810

- ⁷⁰ J. A. Knapp, D. M. Follstaedt: *Nucl. Instr. and Meth.*, 182/183, 1981, 1017
- ⁷¹ S. M. Myers, D. M. Follstaedt: *J. Appl. Phys.*, 52, 1981, 6, 4007
- ⁷² S. Suzuki, K. Kuroki, H. Kobayashi, N. Takahashi: *Mater. Transactions JIM*, 33, 1992, 1068
- ⁷³ W. C. Johnson, B. V. Kovacs: *Met. Trans.*, 9A, 1978, 219
- ⁷⁴ D. Kohler: *J. Appl. Physics Suppl.*, 31, 1960, 5, 408S
- ⁷⁵ C. G. Dunn, J. L. Walter: *Trans. AIME*, 224, 1962, 518
- ⁷⁶ J. J. Kramer: *Met. Trans.*, 23A, 1992, 1987
- ⁷⁷ H. C. Fiedler: *J. Magnetism a. Magnetic Materials*, 26, 1982, 22
- ⁷⁸ G. Lyudkovsky, P. K. Rastogi: *Met. Trans.*, 15A, 1984, 257
- ⁷⁹ G. Lyudkovsky: *IEEE Trans. Magnetics. vol. Mag.*, 22, 1986, 5, 508
- ⁸⁰ B. L. King: *Phil. Trans. R. Soc. Lond.*, 295, 1980, 235
- ⁸¹ W. Hartweck, H. J. Grabke: *Scripta Met.*, 15, 1981, 653
- ⁸² A. Ruck, D. Monceau, H. J. Grabke: *Steel Research*, 67, 1996, 240
- ⁸³ H. H. Grabke: *Härtereitechn. Mitteilungen*, 45, 1990, 110-118
- ⁸⁴ A. Ruck, H. J. Grabke: *Effects of Impurities and Tramp Elements in Case Hardening Steels*, ECSC research project, final report, in press
- ⁸⁵ P. A. Restaino, C. J. McMahon, Jr.: *Trans. ASM*, 60, 1967, 699
- ⁸⁶ J. R. Low, Jr., D. F. Stein, A. M. Turkalo, R. P. Laforce: *Trans. AIME*, 242, 1968, 14
- ⁸⁷ J. R. Rellick, C. J. McMahon, Jr.: *Met. Trans.*, 5, 1974, 2439
- ⁸⁸ C. L. Smith, J. R. Low, Jr.: *Met. Trans.*, 5, 1974, 279
- ⁸⁹ H. Ohtani, H. C. Feng, C. J. McMahon, Jr., R. A. Mulford: *Met. Trans.*, 7A, 1976, 87
- ⁹⁰ H. Ohtani, H. C. Feng, C. J. McMahon, Jr., R. A. Mulford: *Met. Trans.*, 7A, 1976, 1123
- ⁹¹ R. A. Mulford, C. J. McMahon, Jr., D. P. Pope, H. C. Feng: *Met. Trans.*, 7A, 1976, 1269
- ⁹² A. K. Cianelli, H. C. Feng, A. H. Ucisik, C. J. McMahon, Jr.: *Met. Trans.*, 8A, 1977, 1059
- ⁹³ J. Yu, C. J. McMahon, Jr.: *Met. Trans.*, 11A, 1980, 277
- ⁹⁴ T. Wada, W. C. Hagel: *Met. Trans.*, 9A, 1978, 691
- ⁹⁵ J. Kameda, C. J. McMahon, Jr.: *Met. Trans.*, 12A, 1981, 31
- ⁹⁶ M. Guttman, P. R. Krahe, F. Abel, G. Amsel, M. Bruneaux, C. Cohen: *Met. Trans.*, 5, 1974, 167
- ⁹⁷ H. J. Grabke, K. Hennesen, R. Möller, W. Wei: *Scripta Met.*, 21, 1987, 1329-1334
- ⁹⁸ R. Viswanathann, S. J. Hudak, Jr.: *Met. Trans.*, 8A, 1977, 1633
- ⁹⁹ R. O. Ritchie: *Met. Trans.*, 8A, 1977, 1131
- ¹⁰⁰ N. Bandyopadhyay, J. Kameda, C. J. McMahon, Jr.: *Met. Trans.*, 14A, 1983, 881
- ¹⁰¹ R. H. Jones, S. M. Bruemmer, M. T. Thomas, D. R. Baer: *Met. Trans.*, 13A, 1982, 241
- ¹⁰² R. H. Jones, M. T. Thomas, D. R. Baer: *Met. Trans.*, 16A, 1985, 123
- ¹⁰³ H. J. Grabke, R. Möller, H. Erhart, S. S. Brenner: *Surf. Interface Anal.*, 10, 1987, 202
- ¹⁰⁴ H. Erhart, H. J. Grabke, R. Möller: *Archiv Eisenhüttenwes.*, 54, 1983, 285
- ¹⁰⁵ H. G. Beyer, H. J. Grabke: *Development of new deep drawing steels by doping with surface active elements*, current ECSC project

ELECTRICAL SHEETS
AND STRIPS